5262–5273 *Nucleic Acids Research, 2007, Vol. 35, No. 15* *Published online 7 August 2007*
doi:10.1093/nar/gkm565

Metal-ion binding and metal-ion induced folding of the adenine-sensing riboswitch aptamer domain

Jonas Noeske[1,2], Harald Schwalbe[2] and Jens Wöhnert[1,*]

[1]Department of Biochemistry, The University of Texas Health Science Center San Antonio, San Antonio, TX-78229, USA and [2]Institute of Organic Chemistry and Chemical Biology, Center of Biomolecular Magnetic Resonance, Johann-Wolfgang-Goethe-University, 60438 Frankfurt/M., Germany

Received May 25, 2007; Revised July 6, 2007; Accepted July 7, 2007

ABSTRACT

Divalent cations are important in the folding and stabilization of complex RNA structures. The adenine-sensing riboswitch controls the expression of mRNAs for proteins involved in purine metabolism by directly sensing intracellular adenine levels. Adenine binds with high affinity and specificity to the ligand binding or aptamer domain of the adenine-sensing riboswitch. The X-ray structure of this domain in complex with adenine revealed an intricate RNA-fold consisting of a three-helix junction stabilized by long-range base-pairing interactions and identified five binding sites for hexahydrated Mg^{2+}-ions. Furthermore, a role for Mg^{2+}-ions in the ligand-induced folding of this RNA was suggested. Here, we describe the interaction of divalent cations with the RNA–adenine complex in solution as studied by high-resolution NMR spectroscopy. Paramagnetic line broadening, chemical shift mapping and intermolecular nuclear Overhauser effects (NOEs) indicate the presence of at least three binding sites for divalent cations. Two of them are similar to those in the X-ray structure. The third site, which is important for the folding of this RNA, has not been observed previously. The ligand-free state of the RNA is conformationally heterogeneous and contains base-pairing patterns detrimental to ligand binding in the absence of Mg^{2+}, but becomes partially pre-organized for ligand binding in the presence of Mg^{2+}. Compared to the highly similar guanine-sensing riboswitch, the folding pathway for the adenine-sensing riboswitch aptamer domain is more complex and the influence of Mg^{2+} is more pronounced.

INTRODUCTION

RNAs are capable of carrying out a multitude of diverse biological functions. Many biologically active RNAs have to adopt intricate 3D structures that rival protein structures in their complexity to be functional in a cellular environment.

Folding of RNA chains into compact globular 3D structures represents a problem. Due to the polyanionic character of the RNA phosphodiester backbone, it inevitably brings negative charges in close proximity to each other. This results in highly unfavorable electrostatic interactions that are anisotropically distributed in the folded form of the RNA. Therefore, divalent metal ions in general and Mg^{2+} with its favorable charge/size ratio in particular (1) play an important role in RNA folding. Mg^{2+}-ions not only stabilize the final structure through either direct coordination (inner sphere contact) with negatively charged groups of the RNA or in a water-mediated interaction (outer sphere contact) with the hexahydrated ion ($Mg(H_2O)_6^{2+}$). They also influence the rate of folding, stabilize folding intermediates or destabilize alternative conformations (2).

Riboswitches control the expression of a significant number of bacterial genes by binding with high affinity and specificity to small metabolite molecules. To achieve the binding specificity and affinity required for their function, the ligand binding or aptamer domains of these RNA elements must fold into intricate tertiary structures. This is illustrated in a number of X-ray structures of aptamer domain/ligand complexes of different riboswitches (3). In many cases, the X-ray structures revealed the presence of defined Mg^{2+}-binding sites.

For instance for the thiamine pyrophosphate (TPP)-sensing riboswitch it was shown that Mg^{2+} binding is absolutely required for TPP binding (4) and cannot be replaced by monovalent ions or Ca^{2+} (5). The X-ray structure of the *thiC* TPP-sensing riboswitch from *Arabidopsis thaliana* bound to TPP reveals that one

*To whom correspondence should be addressed. Tel: ++1 210 567 8781; Fax: ++1 210 567 6595; Email: jewoe@biochem.uthscsa.edu

© 2007 The Author(s)
This is an Open Access article distributed under the terms of the Creative Commons Attribution Non-Commercial License (http://creativecommons.org/licenses/by-nc/2.0/uk/) which permits unrestricted non-commercial use, distribution, and reproduction in any medium, provided the original work is properly cited.

Downloaded from nar.oxfordjournals.org at Stadt und Universitatsbibliothek / Section Medizinische Hauptbibliothek on November 11, 2010

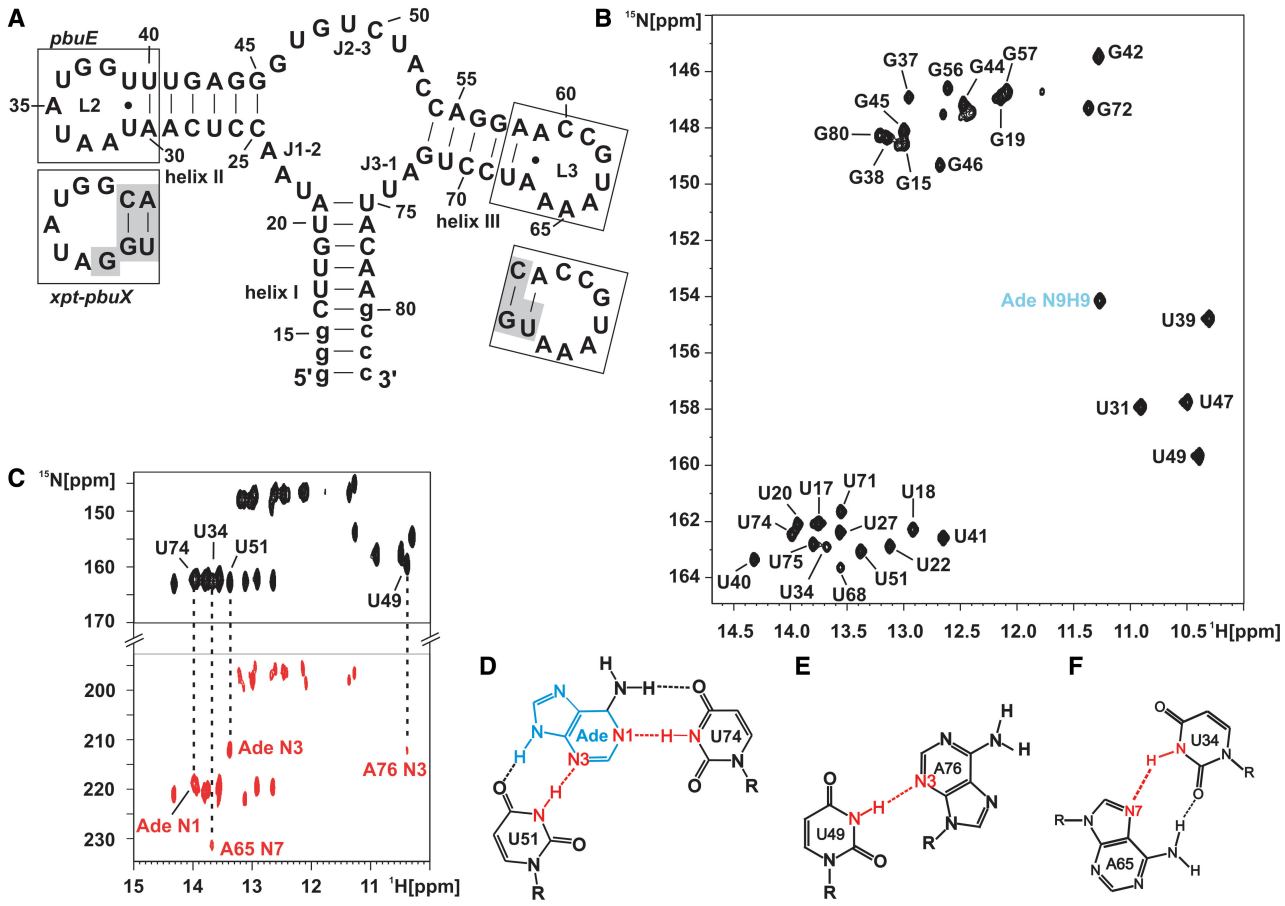

Figure 1. Adenine binding the adenine-sensing riboswitch and complete imino resonance assignment. (**A**) Secondary structure of the aptamer domain of the *pbuE* adenine-sensing riboswitch from *B. subtilis* where loops L2 and L3 are boxed. The sequence of L2 and L3 of the *xpt–pbuX* guanine-sensing riboswitch from *B. subtilis* is shown below in separate boxes. Nucleotides that are different in the guanine-sensing riboswitch compared to the adenine-sensing riboswitch are shaded in gray. (**B**) Imino region of a $^{1}H,^{15}N$-HSQC spectrum of the aptamer domain of the adenine-sensing riboswitch RNA in complex with adenine and complete imino resonance assignment in the absence of Mg^{2+} at 10°C. The signal of the H9N9 imino group of adenine is labeled in blue. (**C**) HNN-COSY experiment of the RNA–adenine complex in the absence of Mg^{2+} at 10°C. The correlation from the hydrogen bond donor (N-H, black resonances) to the hydrogen bond acceptor (N, red resonances) is indicated by dashed lines for RNA–adenine intermolecular hydrogen bonds and for selected tertiary interactions. Schematic drawing of the intermolecular base triple (**D**) involving adenine recognition by U74 and U51 from the adenine-sensing riboswitch, (**E**) the interaction between U49 and A76, and (**F**) the long-range reversed-Hoogsteen A65:U34 base pair. All hydrogen bonds are indicated by dashed lines. Hydrogen bonds including the hydrogen bond donor and the hydrogen bond acceptor which are detected and annotated in (C) are shown in red. The adenine ligand is shown in blue.

Mg^{2+}-ion chelates oxygen atoms in the pyrophosphate moiety of TPP and links them to the RNA whereas there are two bridging Mg^{2+}-ions in the X-ray structure of the *thiM* TPP-sensing riboswitch from *Escherichia coli* bound to TPP. The presence of bridging Mg^{2+}-ions in the X-ray structures is consistent with the strict Mg^{2+} requirements for TPP binding to the TPP-sensing riboswitch (6–8). In contrast, the GlmS riboswitch—a ribozyme that undergoes a self-cleavage reaction in the presence of glucosamine-6-phosphate (GlcN6P)—does not strictly require Mg^{2+} for the self-cleavage reaction. Here, Mg^{2+} can be substituted by either other divalent metal ions or $Co(NH_3)_6^{3+}$ and to some extend by high concentrations of monovalent ions (9) indicating that the metal ion is not involved in catalysis but only in electrostatic stabilization of the structure consistent with the X-ray structure of this complex (10).

The purine-sensing riboswitches are among the smallest riboswitches found so far. All purine riboswitches fold into a three-way junction (Figure 1A) where central structural elements such as the ligand-binding core region and the loops L2 and L3 that cap helices II and III, respectively, show a very high degree of sequence conservation. However, despite the sequence conservation and similarity in structure, the adenine-sensing riboswitch binds adenine with high specificity while the guanine-sensing riboswitch binds guanine. This specificity is mediated by a single nucleotide in the ligand-binding core region which is a cytidin in the guanine-sensing riboswitch and a uridine in the adenine-sensing riboswitch (11,12). It was shown that the purine ligand is bound to this specific nucleotide in the core region by forming an intermolecular Watson–Crick base pair (13–15).

Downloaded from nar.oxfordjournals.org at Stadt und Universitatsbibliothek / Section Medizinische Hauptbibliothek on November 11, 2010

The importance of Mg^{2+}-ions for ligand binding to these riboswitches is less clear. Thermodynamic studies of ligand binding supported a requirement for the presence of Mg^{2+} in the case of hypoxanthine binding to the guanine-sensing riboswitch (16) and FRET studies of the *pbuE* adenine-sensing riboswitch from *B. subtilis* suggested an important role for Mg^{2+} in ligand binding (17). Specifically, Mg^{2+} was required for the formation of the long-range base-pairing interactions between nucleotides in loop 2 and 3. Furthermore, the X-ray structure of the adenine-sensing riboswitch bound to adenine revealed five well-defined Mg^{2+}-binding sites (14) whereas 11 bound $Co(NH_3)_6^{3+}$-ions were found in the X-ray structure of the guanine-sensing riboswitch in complex with hypoxanthine (13). In contrast, NMR studies found ligand binding to be independent of the presence of Mg^{2+} for both the adenine and the guanine-sensing riboswitch (14,15). In addition, in the *xpt–pbuX* guanine-sensing riboswitch from *B. subtilis* the loop–loop interaction between loops 2 and 3 is preformed in the free form of the riboswitch and becomes strengthened in the presence of Mg^{2+} but is stable enough to exist even outside the context of the riboswitch (18). Given the high degree of sequence identity between the guanine- and adenine-sensing riboswitch (Figure 1A) the requirement for Mg^{2+} for the formation of the loop–loop interactions in the adenine-sensing riboswitch as reported in the FRET studies (17) is surprising.

Specifically, with respect to the loop sequences the guanine- and the adenine–sensing riboswitch differ only at the position 32 (Figure 1A) in loop 2. At position 32, the guanine-sensing riboswitch bears a guanosine whereas it is an adenosine in the adenine-sensing riboswitch. The X-ray structures of both riboswitches show that the purine at position 32 stacks between the apical closing base pair of helix II and A33 without making any stabilizing hydrogen bonds and that the residue at position 62 loops out into the solvent (13,14). In addition, there are differences in the closing base pairs of helices II and III in the two riboswitches. The base pair adjacent to loop 2 is an asymmetric U:U base pair in the adenine-sensing riboswitch and a Watson–Crick G:C base pair in the guanine-sensing riboswitch. The closing base pair of helix III is a non-canonical A:A base pair in the adenine-sensing riboswitch but a Watson–Crick A:U base pair in the guanine-sensing riboswitch.

The reported discrepancies in the behavior of the closely related adenine- and guanine-sensing riboswitches prompted us to investigate the binding of divalent metal ions to the *pbuE* adenine-sensing riboswitch and their influence on ligand-induced RNA folding in solution by high-resolution NMR methods in this study.

MATERIALS AND METHODS

Purine ligand synthesis

^{15}N,^{13}C-labeled adenine was synthesized as described in (15). The ligand concentration was determined by UV absorbance at 261 nm using an extinction coefficient $\varepsilon = 13\,400\,mol^{-1}\,cm^{-1}$ (19).

RNA preparation

Labeled RNAs were prepared by *in vitro* transcription with T7 RNA polymerase from linearized plasmid DNA templates using ^{15}N- and ^{15}N,^{13}C-labeled nucleotides purchased from Silantes (Munich, Germany). The labeled RNA was purified as described (20) and concentrations were determined by UV absorbance at 260 nm. The RNA was folded into a homogenous monomeric conformation through denaturation at 363 K for 5 min and rapid cooling to 273 K by 10-fold dilution with ice-cold H_2O. Folding into a homogenous monomeric form was verified by native PAGE (data not shown). The RNA was subsequently exchanged into NMR buffer (25 mM KPO_4, pH 6.2, 50 mM KCl) using Centricon-10 microconcentrators.

NMR spectroscopy

All NMR experiments were recorded on Bruker NMR spectrometers operating at 600, 700, 800 and 900 MHz equipped with a 5 mm HCN cryogenic probes and *z*-axis gradients. The spectra were recorded and processed using Bruker X-WIN NMR3.5 and TopSpin2.0 and were analyzed using XEASY (21). All NMR spectra were recorded at a temperature of 283 K in 90% H_2O/10%D_2O in NMR buffer (25 mM KPO_4, pH 6.2, 50 mM KCl). Water suppression was achieved using the WATERGATE water suppression scheme (22) including water flip back pulses (23). ^{1}H,^{15}N-HSQC, $^{2}J_{HN}$-^{1}H,^{15}N-HSQC (24) and 2D- or ^{15}N-edited 3D-NOESY experiments were performed using standard pulse sequences (25). The $^{2h}J_{NN}$-HNN-COSY experiments (26) were performed as described previously (15).

Cation titrations and Mg^{2+}-binding affinity studies

Titrations of the RNA with Mg^{2+}, Mn^{2+} and $Co(NH_3)_6^{3+}$ were performed directly in the NMR tube by adding aliquots from 125 mM or 500 mM $MgCl_2$, 1 mM $MnCl_2$ or 100 mM $Co(NH_3)_6Cl_3$ stock solutions. The equilibrium binding constant for Mg^{2+} to the RNA was measured by the chemical shift perturbation (CSP) of the imino group of G37. CSPs were calculated using the formula $\sqrt{((\Delta_H)^2 + (\Delta_N/5)^2)/2}$ and were correlated with the ratio of [Mg^{2+}]/[RNA]. Non-linear regression using SigmaPlot9.0 was performed using the following fitting function:

$$f(x) = \frac{b}{2} * \left[(x + 1 + a) - \sqrt{\left((x + 1 + a)^2 - 4x\right)} \right],$$

where $f(x)$ is the CSP at its corresponding ratio x = [Mg^{2+}]/[RNA]. a and b are the fitted parameters where a is the ratio of the dissociation constant (K_D) to [RNA] and b is the CSP for infinite Mg^{2+} concentrations (27).

RESULTS

Adenine binding to the adenine-sensing riboswitch and NMR assignment in solution

The imino region of the ^{1}H,^{15}N-HSQC of the aptamer domain of the adenine-sensing riboswitch in the absence

Downloaded from nar.oxfordjournals.org at Stadt und Universitatsbibliothek / Section Medizinische Hauptbibliothek on November 11, 2010

of Mg^{2+} shows well-resolved and sharp signals in the presence of 1.2 equivalents adenine (Figure 1B). The presence of a signal for the N9H9 imino group of the adenine ligand, which is undetectable in its free form indicates the formation of a high-affinity RNA–ligand complex in the absence of Mg^{2+}. By analyzing 2D-^{1}H,^{1}H-NOESY and 3D-^{1}H,^{1}H,^{15}N-NOESY-HSQC experiments (data not shown) the imino resonances of the RNA–adenine complex could be assigned. The sequence of the aptamer domain of the riboswitch RNA contains 16 guanosine and 19 uridine nucleotides (Figure 1A). For 12 of the guanosine and 17 of the uridine nucleotides imino resonances are detectable in the ^{1}H,^{15}N-HSQC spectrum at 10°C. Imino resonances that could not be assigned correspond to residues G13, G14, U36, G48, G62 and U63. Imino resonances of terminal nucleotides such as G13 and G14 in RNA helices are often not detectable in NMR spectra due to their reduced stability and the resulting fast exchange of the imino proton with the bulk water solvent. The imino groups of residues U36, G48, G62 and U63 are solvent exposed according to the X-ray structure of the adenine–RNA complex (14) which also renders them undetectable due to fast exchange with the bulk water solvent.

The binding mode of adenine to the adenine-sensing riboswitch RNA and tertiary structure characteristics of the adenine–RNA complex were further elucidated by an HNN-COSY experiment (26) which detects hydrogen bonds of the type N-H. . .N. In the HNN-COSY spectrum of the adenine-sensing riboswitch in complex with adenine (Figure 1C), the imino groups of U74 and of U51 show correlations with the N1 and the N3 nitrogen of the bound adenine, respectively. U74, U51 and adenine form an intermolecular base triple (Figure 1D) as observed previously for a mutant of the adenine-sensing riboswitch aptamer domain (15) and in the X-ray structure of the adenine-sensing riboswitch RNA in complex with adenine crystallized in the presence of 200 mM Mg^{2+} (14). Furthermore, several non-canonical base pairings and tertiary interactions can be identified in the HNN-COSY or the NOESY spectra. In the HNN-COSY spectrum, the imino group of U49 is correlated to an adenosine N3 as identified by its chemical shift which is consistent with the hydrogen bond between the U49 imino group and the N3 of A76 in the X-ray structure (Figure 1E). The imino group of U34 shows a correlation to the N7 nitrogen of an adenosine as expected for the reversed Hoogsteen A65:U34 base pair (28) (Figure 1F) observed in the X-ray structure. Nuclear Overhauser effect (NOE) data and the chemical shifts of the C2 and C4 carbonyl groups of U31 and U39 indicate that these nucleotides form an asymmetric U:U base pair (data not shown) (29) also in agreement with the X-ray structure.

In summary, the number of observed imino proton signals, the obtained assignments, the observed intra- and intermolecular NOEs, the binding mode of adenine to the RNA as deduced from the HNN-COSY experiment as well as the observed tertiary non-canonical base-pairing interactions strongly indicate that the teriary structure of the adenine-sensing riboswitch aptamer domain bound to adenine in solution in the absence of Mg^{2+}-ions is virtually identical to the corresponding X-ray structure obtained in the presence of high concentrations of Mg^{2+}. Therefore, the presence of Mg^{2+}-ions is not a prerequisite for either ligand binding or for the correct folding of this RNA–ligand complex.

Divalent cation-binding sites in the adenine–RNA complex in solution

We applied three different but complementary techniques to characterize divalent metal binding to the adenine–RNA complex and to analyze possible structural effects in solution by NMR spectroscopy. First, we observed CSPs in Mg^{2+}-titration experiments caused by the interaction of the metal ion with the RNA–ligand complex. Second, we used the Mn^{2+}-ion as a paramagnetic Mg^{2+}-analog to observe paramagnetic line broadening for NMR signals in close proximity to putative divalent metal-binding sites. Third, we utilized the $[Co(NH_3)_6]^{3+}$-ion which is considered to be an analog of an hexahydrated Mg^{2+}-ion in CSP and NOE experiments to identify imino groups spatially close to putative divalent metal-binding sites.

We titrated the adenine-sensing riboswitch RNA–adenine complex with Mg^{2+} and compared the imino group region of the ^{1}H,^{15}N-HSQC spectrum (Figure 2A). The number of the imino resonances remains unchanged and no large chemical shift changes are observed. This indicates that the overall structure of the complex is not perturbed upon Mg^{2+} binding and that no new structural elements are formed. However, while some imino resonances show no or only small CSP other resonances showed significant CSP upon addition of 5 mM Mg^{2+} to the adenine–RNA complex. Such significant CSPs were observed for U22, G37, G38, U39, U47, U71 and the adenine N9H9 imino group. When these imino groups are mapped on the X-ray structure of the complex, four well-defined areas are visible which are affected by Mg^{2+} binding (Figure 3A). G37 and G38 are located in loop L2 and are involved in the loop–loop interaction forming long-range Watson–Crick base pairs with C61 and C60 in L3, respectively. U39 is located at the apical tip of helix II, U71 is situated in the lower half of helix III pointing to the core region whereas U22, U47 and the adenine N9H9 imino group are all at the interface of the RNA and the bound ligand.

Due to enhanced spin relaxation binding of the paramagnetic Mn^{2+}-ion leads to line broadening of resonances in close proximity to the ion with a distance dependence of $1/r^6$ (30). Only micromolar concentrations of Mn^{2+} are required to induce the effect (31–34). In the RNA–adenine complex in the presence of 5 mM Mg^{2+} imino resonances that show significant line broadening upon titration with 15 μM Mn^{2+} are those of U22, G37, G38, G44, G46, U47, G56, U71 and G72 (Figure 2B). Except for U39 and the N9H9 group of the bound ligand all the resonances that show significant CSP in the Mg^{2+} -titrations also show paramagnetic line broadening induced by the presence of Mn^{2+}. Of the four resonances that show line broadening but no CSP G56 and G72 are close in space to U71 that is affected by both ions. Similarly, G46 where only line broadening is observed is

Downloaded from nar.oxfordjournals.org at Stadt und Universitatsbibliothek / Section Medizinische Hauptbibliothek on November 11, 2010

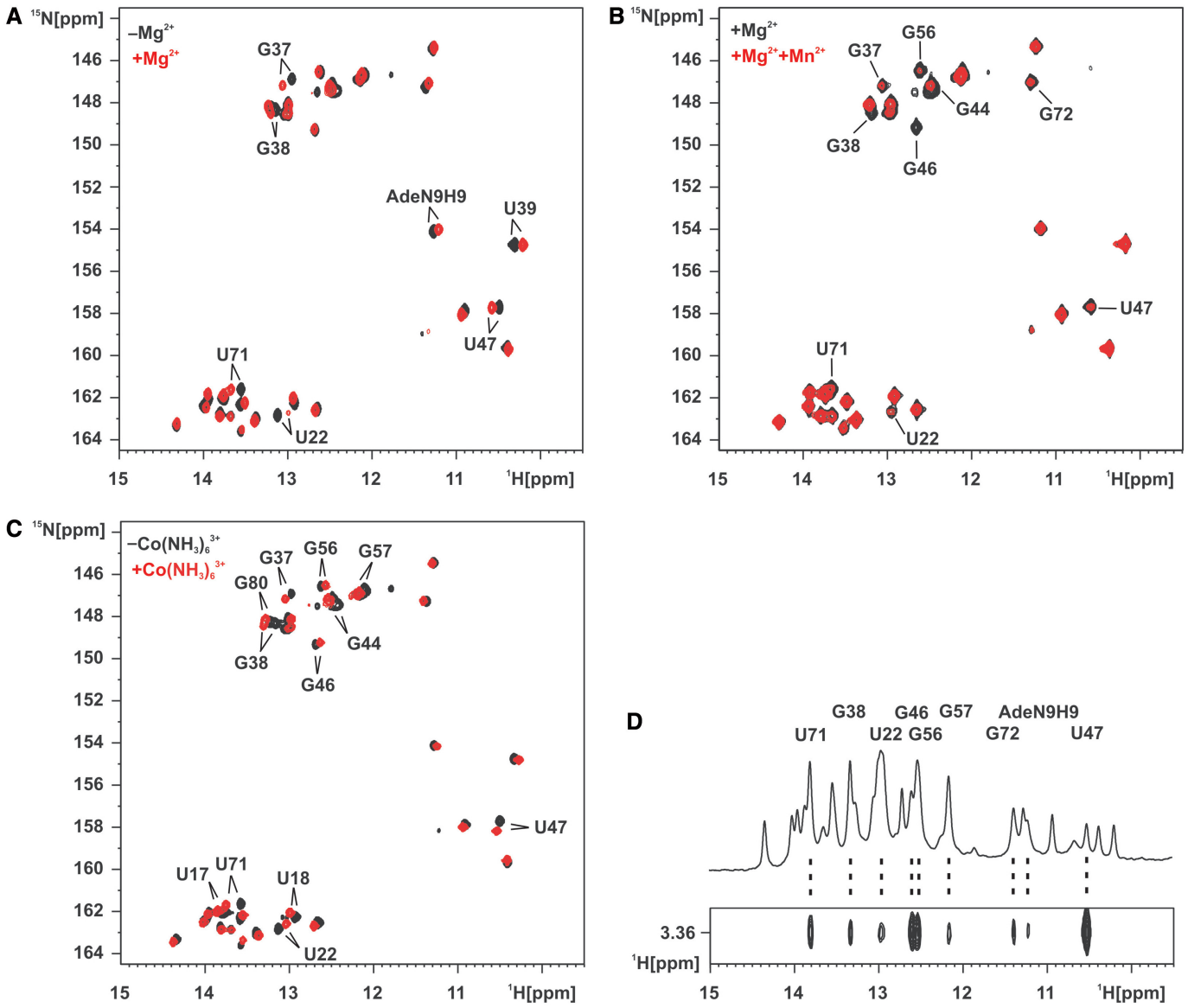

Figure 2. Divalent metal cation binding to the adenine-sensing riboswitch RNA in complex with adenine. (**A**) Overlay of the imino region of a ^{1}H,^{15}N-HSQC spectrum of the aptamer domain of the adenine-sensing riboswitch RNA in complex with adenine in the absence of Mg^{2+} (black) and in the presence of 5 mM Mg^{2+} (red). Imino resonances that experience chemical shift perturbation >0.05 p.p.m. in ^{1}H or >0.4 p.p.m. in ^{15}N upon addition of 5 mM Mg^{2+} are labeled. (**B**) Overlay of the imino region of a ^{1}H,^{15}N-HSQC spectrum of the aptamer domain of the adenine-sensing riboswitch RNA in complex with adenine and 5 mM Mg^{2+} in the absence of Mn^{2+} (black) and in the presence of 15 µM Mn^{2+}. Imino resonances that experience line broadening by the paramagnetic Mn^{2+} are labeled. (**C**) Overlay of the imino region of a ^{1}H,^{15}N-HSQC spectrum of the aptamer domain of the adenine-sensing riboswitch RNA in complex with adenine in the absence of $Co(NH_3)_6^{3+}$ (black) and in the presence of 3 mM $Co(NH_3)_6^{3+}$ (red). Imino resonances that experience chemical shift perturbation >0.05 p.p.m. in ^{1}H or >0.4 p.p.m. in ^{15}N upon addition of 3 mM $Co(NH_3)_6^{3+}$ are labeled. (**D**) Imino region of a 1D-^{1}H spectrum of the aptamer domain of the adenine-sensing riboswitch RNA in complex with adenine in the presence of 5 mM $Co(NH_3)_6^{3+}$ (top) and a section of a 2D-^{1}H,^{1}H-NOESY spectrum showing intermolecular NOEs between the protons of the bulk $Co(NH_3)_6^{3+}$ and the RNA as well as the adenine ligand imino groups (bottom). RNA and adenine ligand imino groups that show intermolecular contacts to the $Co(NH_3)_6^{3+}$ protons are labeled.

adjacent to U47 sensitive to both ions. The residues showing Mn^{2+}-induced line broadening are clustered in four distinct regions when mapped onto the structure (Figure 3B). Three of those regions were previously identified in the Mg^{2+} -titrations. These regions are close to G37 and G38 involved in the loop–loop interaction, the center of helix III (U71, G56 and G72) and in the ligand-binding core (U22, G46 and U47), respectively. G44 located in the lower half of helix II does not show CSP upon titration with Mg^{2+} and is not close in space to other residues that are affected by the presence of either Mg^{2+} or Mn^{2+}.

$Co(NH3)_6^{3+}$ has a geometry similar to the hexahydrated $Mg(H_2O)_6^{2+}$-ion. However, the ligand shell of amino groups is inert to exchange and in contrast to Mg^{2+} cannot form inner sphere contacts (35). In order to complement our magnesium-binding studies we used the adenine–RNA complex and performed

Downloaded from nar.oxfordjournals.org at Stadt und Universitatsbibliothek / Section Medizinische Hauptbibliothek on November 11, 2010

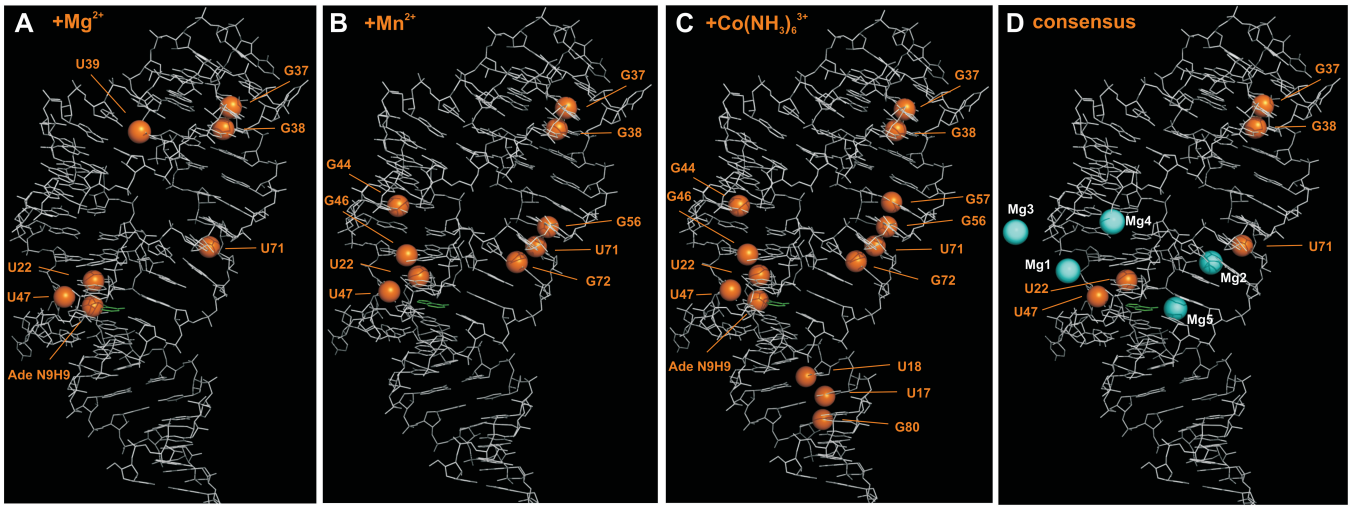

Figure 3. Divalent metal cation-binding sites in solution mapped on the X-ray structure of the closely related *add* adenine-sensing riboswitch from *V. vulnificus* in complex with adenine. (**A**) Imino groups showing chemical shift perturbation upon Mg^{2+} addition in Figure 2A are represented as orange spheres. There are four regions affected that are located in the ligand-binding core, in the loop–loop interaction, at the apical tip of helix II, and in the center of helix III. (**B**) Imino groups showing line broadening by paramagnetic Mn^{2+} in Figure 2B are represented as orange spheres. There are four regions affected that are located in the ligand-binding core, in the loop–loop interaction, and in the center of helix II and helix III. (**C**) Imino groups showing chemical shift perturbation upon $Co(NH_3)_6^{3+}$ addition in Figure 2C and imino groups showing intermolecular NOE contacts to $Co(NH_3)_6^{3+}$ in Figure 2D are represented as orange spheres. There are five regions affected that are located in the ligand-binding core, the loop–loop interaction, and in the center of helix I, helix II and helix III. (**D**) Consensus of imino groups that exhibit all, chemical shift perturbation upon Mg^{2+} addition, line broadening by paramagnetic Mn^{2+}, chemical shift perturbation by as well as intermolecular contacts to $Co(NH_3)_6^{3+}$ are represented as orange spheres. Mg^{2+}-ions found in the X-ray structure are shown as cyan spheres and labeled as in (14). Mg3 is involved in crystal packing. The RNA is drawn in white lines; the adenine ligand is drawn in green lines.

$Co(NH_3)_6^{3+}$ -titration experiments. As for the Mg^{2+} -titration of the complex, the overall conformation of the RNA–ligand complex remained unperturbed and no additional structural elements are formed as indicated by the constant number of observable imino resonances. In a $^{1}H,^{15}N$-HSQC spectrum the imino resonances of U17, U18, U22, G37, G38, G44, G46, U47, G56, G57, U71 and G80 showed significant CSP upon addition of 3 mM $Co(NH_3)_6^{3+}$ (Figure 2C).

The binding site of $Co(NH_3)_6^{3+}$ to the RNA–adenine complex cannot only be studied by CSP but also by intermolecular NOEs between the protons of the NH_3-groups of $Co(NH_3)_6^{3+}$ and RNA protons in spatial proximity. $Co(NH_3)_6^{3+}$ in contrast to $Mg(H_2O)_6^{2+}$ is suitable for such NMR experiments since the hydrogens of the ammonia ligands of $Co(NH_3)_6^{3+}$ exchange slowly with the bulk solvent water and are therefore detectable by NMR. We recorded a 2D-$^{1}H,^{1}H$-NOESY spectrum for the adenine–RNA complex in the presence of 5 mM $Co(NH_3)_6^{3+}$ in which we detected intermolecular NOEs from the protons of $Co(NH_3)_6^{3+}$ to imino group protons of U22, G38, G46, G47, G56, G57, U71, G72 and the N9H9 imino group of the bound adenine (Figure 2D). The residues showing either significant CSP upon the addition of 3 mM $Co(NH_3)_6^{3+}$ or having an intermolecular NOE in the presence of 5 mM $Co(NH_3)_6^{3+}$ include all the residues affected by paramagnetic line broadening in the presence of Mn^{2+}-ions. G57 which only shows NOEs and CSP to $Co(NH_3)_6^{3+}$ but no Mn^{2+}-induced line broadening is located in the center of helix III close to G56, U71 and G72 that are affected by both the presence of $Co(NH_3)_6^{3+}$ and Mn^{2+}. Similarly, the N9H9 group of the bound adenine which displays an NOE to $Co(NH_3)_6^{3+}$ and CSP in the presence of Mg^{2+} but no line broadening in the presence of Mn^{2+} is in the ligand-binding core in close proximity to U22, G46 and G47. The imino resonances of U17, U18 and G80 in helix I only showed CSP in the presence of $Co(NH_3)_6^{3+}$ but not in the presence of Mg^{2+} and no line broadening in the presence of Mn^{2+}-ions.

Mapping of the imino groups experiencing CSP and showing NOEs in the presence $Co(NH_3)_6^{3+}$ on the X-ray structure reveals five distinct binding sites for $Co(NH_3)_6^{3+}$ to the adenine-sensing riboswitch RNA in complex with adenine (Figure 3C).

Three of these binding sites have been identified before in the titration experiments with Mg^{2+} and in the line-broadening experiments with Mn^{2+}. These are located in the vicinity of G37 and G38 in the loop–loop interaction, the center of helix III (U71, G56 and G72) and in the ligand-binding core (U22, G46 and U47), respectively. This is further illustrated by mapping only those imino groups with resonances perturbed by the presence of all three Mg^{2+}-, Mn^{2+}- and $Co(NH_3)_6^{3+}$-ions on the X-ray structure (Figure 3D). One binding site located in the center of helix II is only identified in the line-broadening experiment with Mn^{2+} and by CSP in the presence of $Co(NH_3)_6^{3+}$-ions.

The X-ray structure shows five hexahydrated Mg^{2+}-ions [Mg1 to Mg5, nomenclature of Mg atoms as in (14), Figure 3D] bound to the *add* adenine-sensing riboswitch in complex with adenine (14). One of these Mg^{2+}-binding

Downloaded from nar.oxfordjournals.org at Stadt und Universitatsbibliothek / Section Medizinische Hauptbibliothek on November 11, 2010

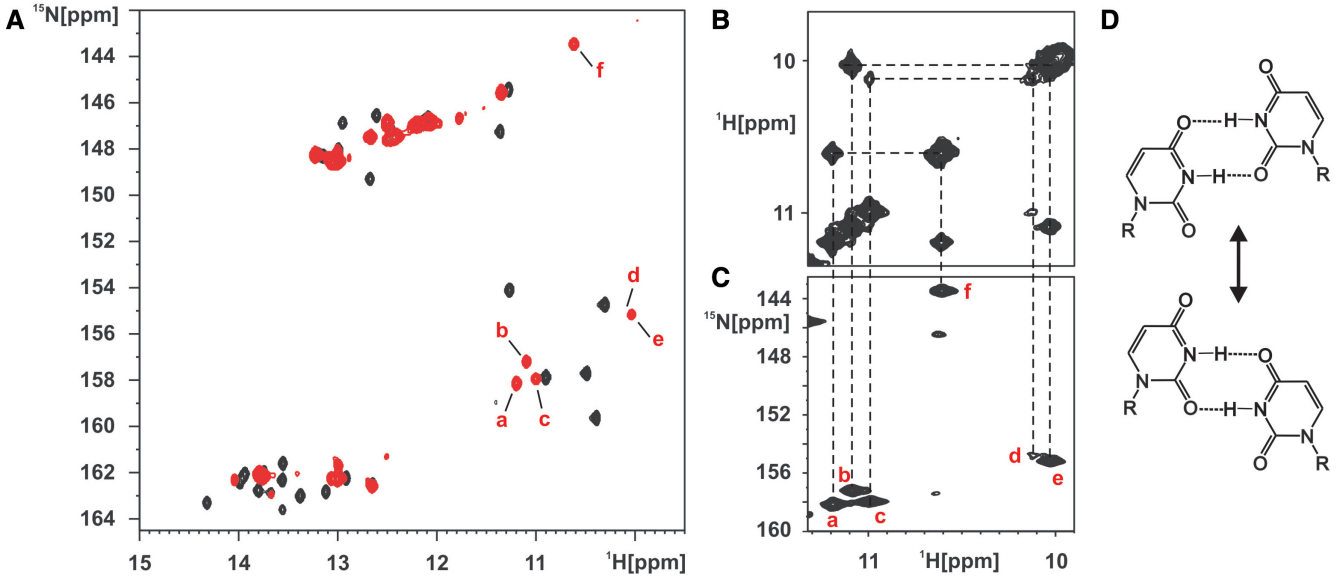

Figure 4. The conformation of the ligand-free adenine-sensing riboswitch RNA in the absence of Mg^{2+}-ions. (**A**) Overlay of the imino region of a $^{1}H,^{15}N$-HSQC spectrum of the free (red) aptamer domain of the adenine-sensing riboswitch RNA in the absence of Mg^{2+} and in complex with adenine (black). Resonances of the five uridines (a–e) and one guanosine (f) imino groups involved in non-canonical base pairing in the free form of the RNA are labeled with red letters. (**B** and **C**) Section of the 2D-$^{1}H,^{1}H$-NOESY spectrum (B) of the free aptamer domain of the adenine-sensing riboswitch RNA and the corresponding region of the $^{1}H,^{15}N$-HSQC spectrum (C). These spectra show the presence of two different U:U base pairs and one G:U base pair in the free form of the RNA. Imino group correlation in the 2D-$^{1}H,^{1}H$-NOESY spectrum (B) are indicate by dashed lines and their identity is revealed by dashed lines to the corresponding resonance in the $^{1}H,^{15}N$-HSQC spectrum (C). (**D**) Two alternative conformations for an asymmetric U:U base pair.

sites (Mg3) is involved in a crystal packing interaction (14). Mg1 in the X-ray structure binds to nucleotides in J2-3 and at the lower end of helix II close to U22 and U47. U22 and U47 have been identified in all four experiments as proximal to a divalent metal ion-binding site in solution. Mg2 in the X-ray structure is located close to U71 in helix II that has been identified as a consensus-binding site in solution. Divalent metal ion binding to the lower end of helix II in solution that would correspond to Mg4 in the X-ray structure was only evident in the line-broadening experiments with Mn^{2+} and in the titrations with $Co(NH_3)_6^{3+}$ (G44). Therefore, this Mg^{2+}-ion might bind only weakly.

No divalent cation binding in solution could be detected in the vicinity of the positions for Mg3 where the binding site is formed by crystal packing interactions and Mg5 in the X-ray structure. On the other hand, no bound Mg^{2+} is observed in the X-ray structure in the vicinity of G37 and G38 in the loop–loop interaction where all the solution experiments unambiguously indicate the presence of a divalent cation-binding site. Interestingly, Mg^{2+} binding at this site appears to be important for the formation of the loop–loop interaction in the *pbuE* adenine-sensing riboswitch.

The free form of the adenine-sensing riboswitch RNA is conformationally disordered and heterogeneous

The $^{1}H,^{15}N$-HSQC spectrum of the free form of the adenine-sensing riboswitch RNA in the absence of metal ions shows imino resonances that are broad and that vary largely in intensity (Figure 4A). In comparison with the adenine bound form, the number of signals is significantly smaller in the free state of the RNA. The signals for U20, U22, G45, G46, U47, U49, U51, U71, G72, U74, U75 located in the ligand-binding core and at the ends of the helices facing the core region are completely absent. This indicates that there are no stabilizing hydrogen-bond interactions between nucleotides in the core region and the core region apparently is largely disordered. In addition, the signal for the imino group of G38 is absent and those of G37 and U34 are barely detectable. This indicates that the loop–loop interaction between loop 2 and loop 3 is strongly destabilized in the free form of the RNA. Only a minor part of the RNA apparently samples a conformation where the two loops interact in exchange with totally open conformations.

However, besides the signals of imino groups belonging to nucleotides in stable Watson–Crick base pairs in the central regions of helices I, II and III, respectively, there are five uridine imino resonances and one guanosine imino resonance with chemical shifts indicating involvement in non-canonical base-pairing interactions. NOEs observed between these imino resonances (Figure 4B) in conjunction with the $^{1}H,^{15}N$-HSQC-spectrum (Figure 4C) suggest the presence of two asymmetrical U:U base pairs and of one G:U wobble base pair in the free RNA. However, there is only one asymmetrical U:U base pair (U31:U39) observed in the adenine bound form of the RNA. In addition, there is no evidence for the presence of a stable G:U wobble base pair in the adenine bound RNA. The second U:U base pair and the G:U wobble base pair therefore represent an alternative base-pairing pattern

Downloaded from nar.oxfordjournals.org at Stadt und Universitatsbibliothek / Section Medizinische Hauptbibliothek on November 11, 2010

unique to the free form of the RNA and have to dissociate in the process of ligand binding. The location of these alternative base pairs either in the loops 2 and 3 or the ligand-binding core cannot unambiguously be established due to the lack of NOEs to other imino protons. In addition, the presence of the second U:U base pair could be either due to an alternative conformation for the U:U base pair between U31 and U39 (Figure 4D) or due to an additional long-range U:U base-pairing interaction. In the first case, exchange cross peaks should be observable between the uridine imino resonances involved in the U:U base-pairing interactions. Unfortunately, both the proton and the ^{15}N chemical shifts of the uridine imino resonances are very similar and such cross peaks would be obscured by the strong diagonal peaks in either ^{1}H,^{1}H-NOESY spectra and ^{15}N-ZZ-exchange experiments (36). However, Mg^{2+}-titration experiments of the free RNA suggest that the alternative G:U and U:U base pairs are located in the region of the loop–loop interaction and compete with the proper formation of the long-range base pairs between loops 2 and 3.

Mg^{2+}-induced conformational changes in the free adenine-sensing riboswitch RNA

We titrated the free form of the adenine-sensing riboswitch RNA with Mg^{2+} and observed changes in the signals of the imino groups in a ^{1}H,^{15}N-HSQC spectrum. The overall number of imino residues decreases and the resonances reach equal intensities in the presence of 5 mM Mg^{2+} (Figure 5A). During the stepwise addition of Mg^{2+}-ions a signal for the imino group of G38 becomes observable and signals for G37 and U34 strongly increase in intensity. This indicates that the presence of Mg^{2+} promotes the formation of the long-range base-pairing interactions between loops 2 and 3. The signals for G37 and G38 continuously shift upon increasing the Mg^{2+} concentration. This suggests that Mg^{2+} shifts the fast equilibrium between open conformations without a loop–loop interaction and closed conformations strongly toward a closed conformation with a stable interaction between loop 2 and loop 3.

At the same time the stepwise addition of Mg^{2+} causes the imino proton signals of the non-canonical G:U wobble base pair and one of the U:U base pairs to disappear whereas the imino protons of the other U:U base pair shift strongly towards chemical shifts similar to those of the adenine bound RNA in the presence of Mg^{2+}. Therefore, the formation of the 'native' stable loop–loop interaction upon addition of Mg^{2+} directly leads to the dissociation of the alternative base pairs observed in the free RNA in the absence of Mg^{2+}. Taken together, these observations indicate that the ensemble of rapidly interconverting conformations observed for the free form of the RNA in the absence of Mg^{2+} converges to a more homogeneous conformation where the loop–loop interaction is present and stable in the presence of Mg^{2+}.

The stepwise CSP of the G37 imino group during the Mg^{2+} -titration was used to estimate the dissociation constant for Mg^{2+} binding to the area of the loop–loop interaction (Figure 5B). G37's imino resonance

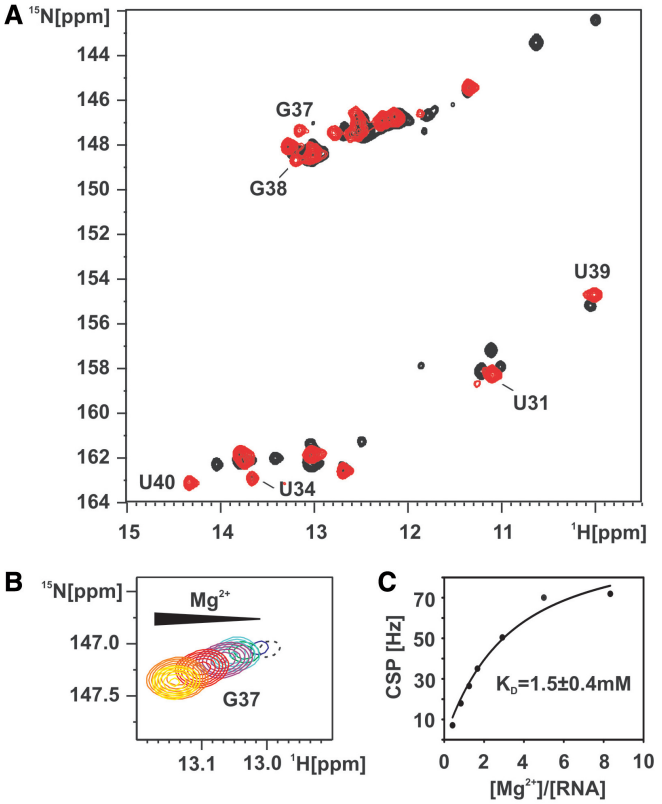

Figure 5. Mg^{2+} induces folding of the loop–loop interaction in the free form of the adenine-sensing riboswitch RNA. (**A**) Overlay of the imino region of a ^{1}H,^{15}N-HSQC spectrum of the free (black) and the Mg^{2+} bound form (red) of the aptamer domain of the adenine-sensing riboswitch RNA. G37 is barely detectable in the free form of the RNA but strongly increases in intensity upon addition of 5 mM Mg^{2+}. (**B**) ^{1}H,^{15}N-HSQC spectrum of the imino group of G37 upon titration with Mg^{2+}. Mg^{2+} titration steps are 0 mM (black), 0.25 mM (blue), 0.5 mM (green), 0.75 mM (cyan), 1 mM (purple) 1.75 mM (red), 3 mM (orange) and 5 mM (yellow). The resonance of the G37 imino group at 0mM Mg^{2+} is shown in dashed contours since it is plotted on a lower level compared to all other titration steps. (**C**) The chemical shift perturbation (CSP) of the G37 imino resonance is plotted against the ratio $[Mg^{2+}]/[RNA]$ and fitted by non-linear regression (black line). The derived binding constant (K_D) of Mg^{2+} to G37 is 1.5 ± 0.4 mM.

strongly increases in intensity and shifts subsequently by a total of 0.15 p.p.m. in ^{1}H and 0.35 p.p.m. in ^{15}N during the titration in agreement with a rapidly associating and dissociating complex of Mg^{2+} and RNA. Correlating the CSP for each titration point with the ratio $[Mg^{2+}]/[RNA]$ yielded a saturation curve revealing an equilibrium dissociation constant of 1.5 mM ± 0.4 mM for Mg^{2+} to the loop L2 region after non-linear regression (Figure 5C).

Interestingly, titrations of the free RNA with $Co(NH_3)_6^{3+}$-ions lead to virtually identical results with regard to the formation of the native loop–loop interaction and the destabilization of the alternative base-pairing patterns. Therefore, Mg^{2+} apparently induces the native folding of this RNA purely by using outer-shell coordination.

Downloaded from nar.oxfordjournals.org at Stadt und Universitatsbibliothek / Section Medizinische Hauptbibliothek on November 11, 2010

A mutant stabilizing the loop–loop interaction in the free form

In order to probe the effect of the stability in helix II on the loop–loop formation properties in the free form of the *pbuE* adenine-sensing riboswitch RNA, we introduced a stabilizing mutation in helix II. In this A30G/U40C double mutant the A30:U40 base pair adjacent to the U31:U39 base pair is replaced by a more stable G:C base pair. In fact, the *xpt–pbuX* guanine-sensing riboswitch displays a U:A base pair at position 30–40 like the *pbuE* adenine-sensing riboswitch but in contrast the adjacent base pair facing the loop–loop interaction is a stable canonical G:C base pair in the case of the *xpt–pbuX* guanine-sensing riboswitch and not a weaker non-canonical U:U base pair as the case in the *pbuE* adenine-sensing riboswitch (Figure 1A and Figure 6 inset). The A30G/U40C double mutant binds to adenine in a manner identical to the wild-type RNA (15). The imino group ^{1}H,^{15}N-HSQC spectrum of the free form of the mutant shows significant differences compared to the one of the wild-type. In the mutant imino group resonances for G37 and U34 which are located in the loop L2 and form long-range base pairs with nucleotides in loop L3 are readily detectable (Figure 6) with chemical shifts similar to those in the adenine bound RNA. In addition, only one U:U base pair is detected which can be assigned as the U31:U39 base pair and no signals corresponding to a G:U wobble base pair can be found. These data show that the mutant RNA in contrast to the wild-type RNA can already form a stable native loop–loop interaction in the free form in the absence of Mg^{2+}.

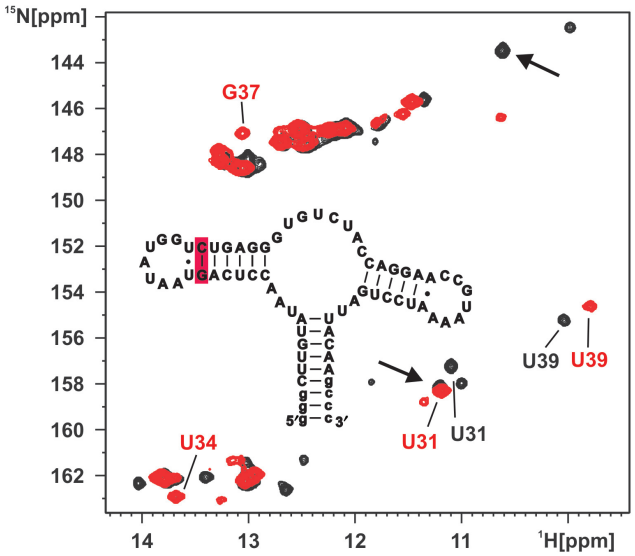

Figure 6. A mutant stabilizing the loop–loop interaction in the free form of the adenine-sensing riboswitch RNA. Overlay of the imino region of a ^{1}H,^{15}N-HSQC spectrum of the free form of the wild-type adenine-sensing riboswitch RNA (black) and a A30G/U40C double mutant of the adenine-sensing riboswitch RNA (red) both in the absence of Mg^{2+}. Signals for the imino groups of G37 and U34 are barely visible in the wild-type RNA but are readily detected in the mutant RNA. Only two signals for the uridine imino groups in an U:U base pair are observable in the mutant. In addition, the imino signals for the wobble G:U base pair (arrows) are absent in the mutant. Inset: Secondary structure of the A30G/U40C double mutant. The mutated base pair at the apical tip of helix II is shaded in red.

DISCUSSION

Divalent cation binding plays a prominent role for RNA folding and stabilization. Mg^{2+}-ions in particular are often required for the proper folding of complex RNA structures giving rise to the notion of an Mg^{2+}-ion-core (37) in highly structured globular RNAs in analogy to the hydrophobic core of protein structures. The X-ray structures of the aptamer domains of the closely related guanine- and adenine-sensing riboswitches are good examples for such intricate globular RNA structures. Not surprisingly, those structures revealed a number of well-defined binding sites for either hexahydrated Mg^{2+}-ions or its structural analog the $Co(NH_3)_6^{3+}$-ion. Furthermore, an important role for Mg^{2+}-ions for the folding and ligand binding of the adenine-sensing riboswitch was reported. On the other hand, our own NMR investigations of the guanine-sensing riboswitch despite revealing a number of well-defined divalent cation-binding sites in solution showed that Mg^{2+} binding was not required for ligand binding and that in the free state of the RNA important tertiary interactions were already pre-organized in a Mg^{2+}-independent manner.

Here, we investigated the binding of divalent cations to the aptamer domain of the *pbuE* adenine-sensing riboswitch in solution and its importance for ligand binding and folding of this RNA. We found that although adenine binding to the aptamer domain is independent of the presence of divalent cations there are a number of well-defined binding sites for divalent cations on the adenine–RNA complex in solution. In contrast to the related guanine-sensing riboswitch, the free state of the adenine-sensing riboswitch is conformationally heterogeneous and displays alternative base-pairing patterns detrimental to ligand binding. The addition of Mg^{2+}-ions induces the formation of a crucial tertiary interaction, the formation of base-pairing interactions between nucleotides in loops 2 and 3, and in turn destabilizes the alternative base pairs thereby pre-organizing the structure of the RNA for ligand binding.

Possible divalent cation-binding sites in solution were identified by using four different techniques: Mg^{2+}-induced CSP, paramagnetic line broadening induced by Mn^{2+}-ions, CSP induced by $Co(NH_3)_6^{3+}$-ions and intermolecular NOEs between $Co(NH_3)_6^{3+}$-ions and RNA protons. Despite differences in their inherent sensitivity these experiments yielded consistent results. Three distinct Mg^{2+}-binding sites were identified in all four experiments. Apparently, in all three binding sites the ion binds through 'outer shell' coordination since Mg^{2+} titrations and $Co(NH_3)_6^{3+}$-binding experiments show similar effects. Two of those binding sites are also seen in the X-ray structure and were also found in solution for the structurally very similar *xpt–pbuX* guanine-sensing riboswitch. The third binding site identified in all experiments was not seen in the X-ray structure. It is located close to nucleotides involved in tertiary base-pairing interactions between the loops 2 and 3.

Downloaded from nar.oxfordjournals.org at Stadt und Universitatsbibliothek / Section Medizinische Hauptbibliothek on November 11, 2010

This is consistent with FRET results showing that Mg^{2+} binding promotes the formation of this loop–loop interaction already in the absence of ligand (17,38) and with our own results that show Mg^{2+}-dependent formation of the tertiary base-pairing interactions between nucleotides in these two loops. A divalent cation-binding site at this position was also identified in solution for the structurally highly similar guanine-sensing riboswitch (18). A fourth possible binding site was only identified in the line-broadening experiments with Mn^{2+} and the $Co(NH_3)_6^{3+}$-binding experiments. Interestingly, this binding site also corresponds to the position of a bound Mg^{2+}-ion in the X-ray structure. Probably the affinity of this site is lower and the magnitude of the Mg^{2+}-induced CSP is too small to identify this site in the Mg^{2+} experiments. Two Mg^{2+}-binding sites found in the X-ray structure (Mg3 and Mg5) were not found in solution. One of those is created by crystal packing interactions (Mg3). In principle, the failure to detect the Mg^{2+}-binding site corresponding to Mg5 (14) of the X-ray structure might be due to our exclusive use of guanosine and uridine imino groups as probes for metal-induced chemical shift changes. This would prevent the detection of metal ion binding in A, C-rich regions of the structure due to the lack of suitable probes. However, Mg5 is close in space to the imino groups of U74 and U75. Thus, our results suggest that this binding site is apparently not or only rarely occupied by a divalent cation in solution.

On the other hand, $Co(NH_3)_6^{3+}$-ions in solution seem to bind to a site in helix I in an area with a high density of uridine carbonyl groups where neither the X-ray structure nor the Mg^{2+}- and Mn^{2+}-titration experiments showed a binding site. Due to their higher charge density $Co(NH_3)_6^{3+}$-ions have an ~10-fold higher affinity (39) than divalent ions and induce larger CSPs than divalent ions so it seems likely that in this experiment a very weak binding site was detected. The value of the $Co(NH_3)_6^{3+}$-ion as a structural mimic of hexahydrated Mg^{2+}-ions has been questioned recently (40). Our results indicate that it is a useful probe as long as ion binding occurs through outer shell coordination but also that exclusive reliance on $Co(NH_3)_6^{3+}$-ions as a probe might lead to an overestimation of the amount of divalent cation binding.

Whereas Mg^{2+} binding does not influence the structure of the RNA–ligand complex it has a significant influence on the conformation of the free state of the adenine-sensing riboswitch. In contrast to our findings for the aptamer domain of the closely related guanine-sensing riboswitch in the absence of Mg^{2+} the free aptamer domain of the *pbuE* adenine-sensing riboswitch studied here does not show a pre-organized stable tertiary interaction between the loops 2 and 3. Instead, an alternative base-pairing pattern is observed that most likely involves loop nucleotides and competes with the formation of this loop–loop interaction and ultimately ligand binding. Mg^{2+} promotes the formation of this crucial tertiary interaction and directly induces the formation of base-pairing interactions between loop 2 and 3 in agreement with the FRET results reported by Lafontaine and co-workers and Micura and coworkers (17,38). Therefore, the small sequence differences in the closing base pairs of helix II and III and loop 2 and 3, respectively, between the guanine and the adenine-sensing riboswitch lead to significant differences in the conformation of the free state of the RNA and a different role for Mg^{2+} in the folding pathway (Figure 7). The stabilization of the loop–loop interaction through either Mg^{2+} binding or more stable base-pairing interactions in helix II as found in the majority of the guanine-sensing riboswitches (12,18) and the resulting pre-organization of the RNA fold might actually have important consequences for the kinetics of ligand binding (k_{on}) which would most likely be faster in the presence of Mg^{2+} or the stabilizing base-pairing interactions. In turn, the 'on' rate of ligand binding is important for the proper function of a 'kinetically' controlled riboswitch such as the *pbuE* riboswitch (41). On the other hand, the base pairing is the same in helix II of the *add* riboswitch from *Vibrio vulnificus* which appears to be thermodynamically controlled (38). In fact, all the adenine-sensing riboswitches described so far (42) contain either at least one non-canonical base pair or two A:U base pairs as closing base pairs of loop 2. In contrast, two Watson–Crick base pairs with either one or even both being a G:C base pair are found at these positions in most of the guanine-sensing riboswitches. Therefore, it is tempting to speculate that the Mg^{2+} concentration might modulate the effectivity of

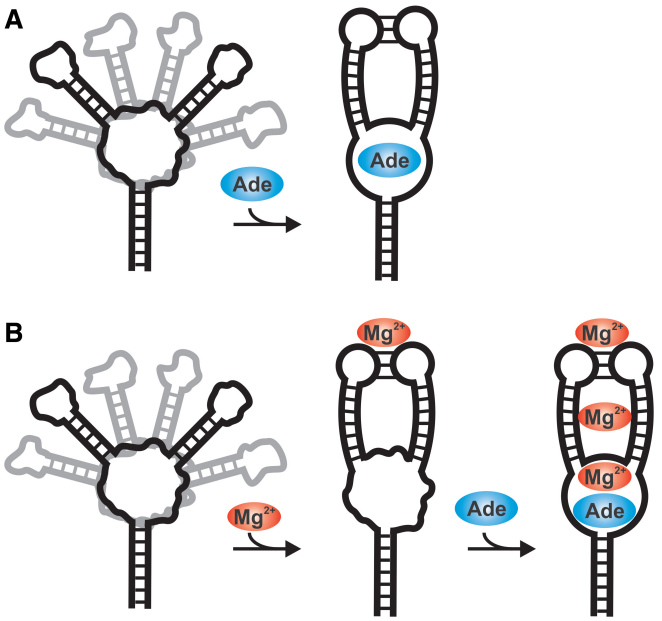

Figure 7. Cartoon of the folding pathway for the adenine-sensing riboswitch RNA upon adenine and/or Mg^{2+} binding. (**A**) In the absence of Mg^{2+} the free form of the RNA is an ensemble of interconverting structures with different interhelical angles. The core region and the loops L2 and L3 are largely unstructured and partially misfolded. Adenine binding simultaneously induces the folding of the core region and the formation of the long-range base-pairing interactions between loop 2 and 3. (**B**) The presence of Mg^{2+} induces the formation of the proper long-range base-pairing interactions between loop II and loop III resulting in a conformation partially pre-organized for adenine binding. The subsequent binding of adenine to the core region yields the fully structured RNA–adenine complex with at least three Mg^{2+}-binding sites.

Downloaded from nar.oxfordjournals.org at Stadt und Universitatsbibliothek / Section Medizinische Hauptbibliothek on November 11, 2010

riboswitch-mediated gene regulation in the case of the adenine-sensing riboswitches.

The detrimental effect for ligand binding of an alternative long-range base-pairing interaction in the core region of the adenine-sensing riboswitch (G48A) has been shown before (42) and the sequence conservation patterns the different variants suggest that they have evolved in a way to minimize this possibility. Here, we demonstrate that the presence of Mg^{2+}-ions apparently helps to avoid an alternative base-pairing pattern in the loop regions. Finally, we demonstrate that small sequence variations can have a profound effect on the folding pathway of this RNA since a slight variation of an apical base pair in helix II is as effective as Mg^{2+} in stabilizing the loop–loop interaction. Similar effects on RNA-folding pathways have been reported for instance for point mutations in the P5abc domain of the *Tetrahymena* group I intron (43,44).

The large influence of small sequence variations on the structure of the free state of the purine-binding riboswitches and their folding pathways might have interesting implications for the design of drugs that are targeted against purine-sensing riboswitches (45). The high similarity of the structures of their aptamer domain ligand complexes will render it difficult to find drugs that bind selectively to only a subset of these riboswitches such as those of a given bacterium. However, targeting the free form of these riboswitches where small sequence differences result in different conformations will allow selectivity. For some of these riboswitches it might be promising to develop inhibitors for the formation of the loop–loop interaction which is essential for ligand binding (13) while those with a stable preformed loop–loop interaction will not be affected in their function.

ACKNOWLEDGEMENTS

We are indebted to C. Richter and E. Stirnal for excellent technical support and H. R. Nasiri for the synthesis of ^{13}C,^{15}N-labeled adenine. We are grateful to M. Görlach and K. Abarca Heidemann for critical reading of the manuscript and their helpful comments. This work was supported by the Deutsche Forschungsgemeinschaft (DFG) through the SFB 579 'RNA-ligand interactions', the Center of Biomolecular Magnetic Resonance (State of Hesse), NIH (RR13879) and by start-up funding from the Department of Biochemistry, University of Texas Health Science Center, San Antonio (USA). J. N. (by a fellowship) and H.S. were supported by the Fonds der Chemischen Industrie. Funding to pay the Open Access publication charges for this article was provided by start-up funds to J. W. from the Department of Biochemistry, The University of Texas Health Science Center San Antonio.

Conflict of interest statement. None declared.

REFERENCES

1. Woodson,S.A. (2005) Metal ions and RNA folding: a highly charged topic with a dynamic future. *Curr. Opin. Chem. Biol.*, **9**, 104–109.
2. Wu,M. and Tinoco,I.Jr (1998) RNA folding causes secondary structure rearrangement. *Proc. Natl Acad. Sci. USA*, **95**, 11555–11560.
3. Schwalbe,H., Buck,J., Furtig,B., Noeske,J. and Wohnert,J. (2007) Structures of RNA switches: insight into molecular recognition and tertiary structure. *Angewandte Chemie International Ed.*, **46**, 1212–1219.
4. Noeske,J., Richter,C., Stirnal,E., Schwalbe,H. and Wohnert,J. (2006) Phosphate-group recognition by the aptamer domain of the thiamine pyrophosphate sensing riboswitch. *Chembiochem*, **7**, 1451–1456.
5. Yamauchi,T., Miyoshi,D., Kubodera,T., Nishimura,A., Nakai,S. and Sugimoto,N. (2005) Roles of Mg^{2+} in TPP-dependent riboswitch. *FEBS Lett.*, **579**, 2583–2588.
6. Edwards,T.E. and Ferre-D'Amare,A.R. (2006) Crystal structures of the thi-box riboswitch bound to thiamine pyrophosphate analogs reveal adaptive RNA-small molecule recognition. *Structure*, **14**, 1459–1468.
7. Serganov,A., Polonskaia,A., Phan,A.T., Breaker,R.R. and Patel,D.J. (2006) Structural basis for gene regulation by a thiamine pyrophosphate-sensing riboswitch. *Nature*, **441**, 1167–1171.
8. Thore,S., Leibundgut,M. and Ban,N. (2006) Structure of the eukaryotic thiamine pyrophosphate riboswitch with its regulatory ligand. *Science*, **312**, 1208–1211.
9. Roth,A., Nahvi,A., Lee,M., Jona,I. and Breaker,R.R. (2006) Characteristics of the glmS ribozyme suggest only structural roles for divalent metal ions. *RNA*, **12**, 607–619.
10. Klein,D.J. and Ferre-D'Amare,A.R. (2006) Structural basis of glmS ribozyme activation by glucosamine-6-phosphate. *Science*, **313**, 1752–1756.
11. Mandal,M., Boese,B., Barrick,J.E., Winkler,W.C. and Breaker,R.R. (2003) Riboswitches control fundamental biochemical pathways in Bacillus subtilis and other bacteria. *Cell*, **113**, 577–586.
12. Mandal,M. and Breaker,R.R. (2004) Adenine riboswitches and gene activation by disruption of a transcription terminator. *Nat. Struct. Mol. Biol.*, **11**, 29–35.
13. Batey,R.T., Gilbert,S.D. and Montange,R.K. (2004) Structure of a natural guanine responsive riboswitch complexed with the metabolite hypoxanthine. *Nature*, **432**, 411–415.
14. Serganov,A., Yuan,Y.R., Pikovskaya,O., Polonskaia,A., Malinina,L., Phan,A.T., Hobartner,C., Micura,R., Breaker,R.R. *et al.* (2004) Structural basis for discriminative regulation of gene expression by adenine and guanine sensing mRNAs. *Chem. Biol.*, **11**, 1729–1741.
15. Noeske,J., Richter,C., Grundl,M.A., Nasiri,H.R., Schwalbe,H. and Wohnert,J. (2005) An intermolecular base triple as the basis of ligand specificity and affinity in the guanine and adenine sensing riboswitch RNAs. *Proc. Natl Acad. Sci. USA*, **102**, 1372–1377.
16. Gilbert,S.D., Stoddard,C.D., Wise,S.J. and Batey,R.T. (2006) Thermodynamic and kinetic characterization of ligand binding to the purine riboswitch aptamer domain. *J. Mol. Biol.*, **359**, 754–768.
17. Lemay,J.F., Penedo,J.C., Tremblay,R., Lilley,D.M. and Lafontaine,D.A. (2006) Folding of the adenine riboswitch. *Chem. Biol.*, **13**, 857–868.
18. Noeske,J., Buck,J., Furtig,B., Nasiri,H.R., Schwalbe,H. and Wohnert,J. (2007) Interplay of 'induced fit' and preorganization in the ligand induced folding of the aptamer domain of the guanine binding riboswitch. *Nucleic Acids Res.*, **35**, 572–583.
19. Fasman,G. (1975) edn. *Handbook of Biochemistry and Molecular Biology, Nucleic Acids, I.* 3rd edn. CRC press.
20. Stoldt,M., Wohnert,J., Ohlenschlager,O., Gorlach,M. and Brown,L.R. (1999) The NMR structure of the 5S rRNA E-domain-protein L25 complex shows preformed and induced recognition. *EMBO J.*, **18**, 6508–6521.
21. Bartels,C., Xia,T.-H., Billeter,M., Güntert,P. and Wüthrich,K. (1995) The program XEASY for computer-supported NMR spectral analysis of biological macromolecules. *J. Biomol. NMR*, **6**, 1–10.
22. Piotto,M., Saudek,V. and Sklenar,V. (1992) Gradient-tailored excitation for single-quantum NMR spectroscopy of aqueous solutions. *J. Biomol. NMR*, **2**, 661–665.
23. Grzesiek,S. and Bax,A. (1993) The importance of not saturating water in protein NMR. Application to sensitivity enhancement and NOE measurements. *J. Am. Chem. Soc.*, **115**, 12593–12594.

Downloaded from nar.oxfordjournals.org at Stadt und Universitatsbibliothek / Section Medizinische Hauptbibliothek on November 11, 2010

24. Sklenar,V., Peterson,R.D., Rejante,M.R. and Feigon,J. (1994) Correlation of nucleotide base and sugar protons in a 15N-labeled HIV-1 RNA oligonucleotide by 1H-15N HSQC experiments. *J. Biomol. NMR*, **4**, 117–122.
25. Wijmenga,S.S. and van Buuren,B.N.M. (1998) The use of NMR methods for conformational studies of nucleic acids. *Prog. Nucl. Magn. Reson. Spectrosc.*, **32**, 287–387.
26. Dingley,A.J. and Grzesiek,S. (1998) Direct observation of hydrogen bonds in nucleic acid base pairs by internucleotide $^{2}J_{NN}$ couplings. *J. Am. Chem. Soc.*, **120**, 8293–8297.
27. Kang,R.S., Daniels,C.M., Francis,S.A., Shih,S.C., Salerno,W.J., Hicke,L. and Radhakrishnan,I. (2003) Solution structure of a CUE-ubiquitin complex reveals a conserved mode of ubiquitin binding. *Cell*, **113**, 621–630.
28. Wohnert,J., Dingley,A.J., Stoldt,M., Gorlach,M., Grzesiek,S. and Brown,L.R. (1999) Direct identification of NH…N hydrogen bonds in non-canonical base pairs of RNA by NMR spectroscopy. *Nucleic Acids Res.*, **27**, 3104–3110.
29. Ohlenschlager,O., Wohnert,J., Bucci,E., Seitz,S., Hafner,S., Ramachandran,R., Zell,R. and Gorlach,M. (2004) The structure of the stemloop D subdomain of coxsackievirus B3 cloverleaf RNA and its interaction with the proteinase 3C. *Structure*, **12**, 237–248.
30. Bertini,I. and Luchinat,C. (1986) *NMR of Paramagnetic Molecules in Biological Systems* Menlo Park, CA, USA.
31. Hurd,R.E., Azhderian,E. and Reid,B.R. (1979) Paramagnetic ion effects on the nuclear magnetic resonance spectrum of transfer ribonucleic acid: assignment of the 15-48 tertiary resonance. *Biochemistry*, **18**, 4012–4017.
32. Allain,F.H. and Varani,G. (1995) Divalent metal ion binding to a conserved wobble pair defining the upstream site of cleavage of group I self-splicing introns. *Nucleic Acids Res.*, **23**, 341–350.
33. Butcher,S.E., Allain,F.H. and Feigon,J. (2000) Determination of metal ion binding sites within the hairpin ribozyme domains by NMR. *Biochemistry*, **39**, 2174–2182.
34. Feigon,J., Butcher,S.E., Finger,L.D. and Hud,N.V. (2001) Solution nuclear magnetic resonance probing of cation binding sites on nucleic acids. *Methods Enzymol.*, **338**, 400–420.
35. Cowan,J.A. (1993) Metallobiochemistry of RNA. $Co(NH_3)_6^{3+}$ as a probe for Mg^{2+}(aq) binding sites. *J. Inorg. Biochem.*, **49**, 171–175.
36. Hud,N.V., Schultze,P., Sklenar,V. and Feigon,J. (1999) Binding sites and dynamics of ammonium ions in a telomere repeat DNA quadruplex. *J. Mol. Biol.*, **285**, 233–243.
37. Cate,J.H., Hanna,R.L. and Doudna,J.A. (1997) A magnesium ion core at the heart of a ribozyme domain. *Nat. Struct. Biol.*, **4**, 553–558.
38. Rieder,R., Lang,K., Graber,D. and Micura,R. (2007) Ligand-induced folding of the adenosine deaminase A-riboswitch and implications on riboswitch translational control. *Chembiochem.*, **8**, 896–902.
39. Gonzalez,R.L.Jr and Tinoco,I.Jr (1999) Solution structure and thermodynamics of a divalent metal ion binding site in an RNA pseudoknot. *J. Mol. Biol.*, **289**, 1267–1282.
40. Fan,Y., Gaffney,B.L. and Jones,R.A. (2005) RNA GG x UU motif binds K^{+} but not Mg^{2+}. *J. Am. Chem. Soc.*, **127**, 17588–17589.
41. Wickiser,J.K., Cheah,M.T., Breaker,R.R. and Crothers,D.M. (2005) The kinetics of ligand binding by an adenine sensing riboswitch. *Biochemistry*, **44**, 13404–13414.
42. Lemay,J.F. and Lafontaine,D.A. (2007) Core requirements of the adenine riboswitch aptamer for ligand binding. *RNA*, **13**, 339–350.
43. Silverman,S.K., Zheng,M., Wu,M., Tinoco,I.Jr and Cech,T.R. (1999) Quantifying the energetic interplay of RNA tertiary and secondary structure interactions. *RNA*, **5**, 1665–1674.
44. Zheng,M., Wu,M. and Tinoco,I.Jr (2001) Formation of a GNRA tetraloop in P5abc can disrupt an interdomain interaction in the Tetrahymena group I ribozyme. *Proc. Natl Acad. Sci. USA*, **98**, 3695–3700.
45. Blount,K.F. and Breaker,R.R. (2006) Riboswitches as antibacterial drug targets. *Nat. Biotechnol.*, **24**, 1558–1564.

Downloaded from nar.oxfordjournals.org at Stadt und Universitatsbibliothek / Section Medizinische Hauptbibliothek on November 11, 2010